대한기계학회 2000년도 춘계학술대회논문집 B pp. 459~464 KSME 00S231

Multiple Orifice Technique for Pressure Drop in Compressible Pipe Flows

Heuydong Kim*, Byoungsoo Koo**, Sunhoon Woo** and Toshiaki Setoguchi***

Key Words : Compressible Flow, Flow Control, Shock Wave, Multiple Orifice, Internal Flow.

Abstract

In order to investigate the effectiveness of an orifice system in producing pressure drops and the effect of compressibility on the pressure drop, computations using the mass-averaged implicit Navier-Stokes equations were applied to the axisymmetric pipe flows with the operating pressure ratio from 1.5 to 20.0. The standard k-e turbulence model was employed to close the governing equations. Numerical calculations were carried out for some combinations of the multiple orifice configurations. The present CFD data showed that the orifice systems, which have been applied to incompressible flow regime to date, can not be used for the high operating pressure ratio flows. The orifice interval did not strongly affect the total pressure drop, but the orifice area ratio more than 2.5 led to high pressure drops. The total pressure drop rapidly increased in the range of the operating pressure ratio from 1.5 to 4.0, but it did not depend on the operating pressure ratio over 4.0.

1. Introduction

Flow through devices such as an orifice, nozzle, venturi, diffuser and bend has been of great interest to designers of flow systems. These devices are often used to change pressure, velocity or direction of fluid flow, and therefore could be regarded as flow control devices. The orifice has a flow control device is of practical importance as it is simple to design and manufacture and is also cost effective. Orifice has a device, which is better understood as an instrument for measurement of flow rates in a flow system.

There have been systematic investigations[1,2,3] of the effects of Reynolds number, heat transfer and geometry on the effectiveness (discharge coefficient) of orifice for flow measurements. However the effect of compressibility on orifice effectiveness is not fully understood.[4,5] There is no knowledge based on the use of orifice as a control device in compressible flow systems.

In recent years the orifice is used to alleviate noise of exhaust flows in power plants and engines by increasing the pressure drop between the source of noise and the ambient.[6,7,8] The objective of this work is to investigate the effectiveness of an orifice in producing pressure drops and the effect of compressibility on the pressure drop by CFD approach.

Computations using the mass-averaged implicit Navier-Stokes equations were applied to the axisymmetric pipe flows operating at a moderate pressure ratio. The governing equations were discretized in space using a finite volume differencing formulation. The standard k-e turbulence model was employed to close the governing equations. Numerical calculations were carried out for some combinations of the multiple orifice configurations.

2. CFD Analysis

It is understood that in a pipe or duct system the flow will choke at a minimum cross-sectional area in pipe, if the ratio of the upstream pressure to the downstream pressure of pipe is sufficiently high. For the multiple orifice pipe, the prediction of the flow choke is not straightforward due to Vena Contraction, large viscous losses between the orifices, and flow unsteadiness. Pressure drop of the flow passing through the multiple orifice system would be strongly dependent on the operating pressure ratio, the orifice configuration, the orifice interval and Reynolds number.

In the present investigation the effects of the operating pressure ratio on the pressure drop across the orifice were studied. The orifice configurations investigated included single and multiple orifices. Figure 1 shows the entire computational domain of the double orifice flow field. The pipe has a diameter of 2R. The flow direction is from left towards right of the pipe. The domain extends about 4R back from the first orifice, which has an opening area of of $\pi r_1^2 (=A_1)$, and about 10R downstream away from the second orifice which has an opening area of of $\pi r_2^2 (=A_2)$. The heights of the two orifices were

* Dept. of Mechanical Eng., Andong Univ.
** Graduate School of Mechanical Eng., Andong Univ.
*** Dept. of Mechanical Eng., Saga Univ., Japan

changed to make different values of A_2/A_1. The interval (l) between orifices was changed in range of l=0.5R to 4.0R, but the pipe length (L) downstream of the second orifice was kept constant for all the present computations. Each orifice plate had 5.0mm thick, and thus the ratio of the orifice plate thickness to the radius of the pipe was so small(t/R=0.05) that the orifice plate thickness had a negligible influence on the flow field under consideration.

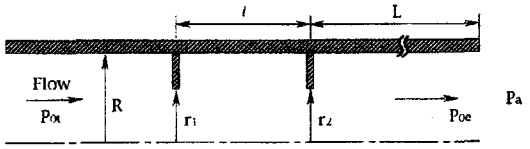

Figure 1. Multiple orifice pipe flow

The configuration studied included a single, double and triple orifice system as will be shown later. The approach pipe length upstream and downstream of the orifice system was kept constant. Generally it is known that structured grid produces a faster convergence of the solution when compared with unstructured grid. Therefore a structured and fine grid was used for the analysis, as shown in Figure 2. The fineness of computational grid required to obtain grid independent solutions was examined for some of the flow fields under consideration.

Figure 2. Computational grid

More than 45 thousands of node points seemed to make no appreciable difference to the results. The computational grids were clustered with finer grids near the wall surfaces and the orifices, and the region around the orifices, only being generated in regions which required higher resolution. Over all of the present computations, the wall y+ values of the grids were held reasonably quite small to facilitate the standard k-e turbulence model incorporated with the standard wall function.

The governing equations used in the numerical scheme are the axisymmetric viscous formulations of mass, momentum, and energy conservation laws. The governing equations are given by the conservation form of the axisymmetric, mass averaged, time-dependent Navier-Stokes equations. The resulting equations are expressed in an integral form for an arbitrary control volume V,

$$\Gamma \frac{\partial}{\partial t} \int_V \boldsymbol{Q}\, dV + \oint [F - G] \bullet dA = 0 \quad (1)$$

where $\boldsymbol{F}$ and $\boldsymbol{G}$ are the inviscid and viscous flux vectors in standard conservation form and $\boldsymbol{Q}$ is the dependent vector of primary variables.

$$\boldsymbol{F} = [\rho v,\ \rho v v_x + p\hat{i},\ \rho v v_y + p\hat{j},\ \rho v v_z + p\hat{k},\ \rho v H]^T$$

$$\boldsymbol{G} = [0,\ \tau_{xi},\ \tau_{yi},\ \tau_{zi},\ \tau_{ij} v_j + q]^T \quad (2)$$

$$\boldsymbol{Q} = [p, v_x, v_y, v_z, T]^T$$

In Eq.(2), H is total enthalpy per unit mass and is related to the total energy E by $H=E+p/\rho$, where E includes both internal and kinetic energy. The preconditioning matrix Γ is included in Eq.(1) to provide an efficient solution of the present axisymmetric compressible flow. This matrix is given by

$$\Gamma = \begin{bmatrix} \theta & 0 & 0 & 0 & \rho_T \\ \theta v_x & \rho & 0 & 0 & \rho_T v_x \\ \theta v_y & 0 & \rho & 0 & \rho_T v_y \\ \theta v_z & 0 & 0 & \rho & \rho_T v_z \\ \theta H - \delta_1 & \rho v_x & \rho v_y & \rho v_z & \rho_T H + \rho C_p \end{bmatrix} \quad (3)$$

where ρ_T is the derivative of density with respect to temperature at constant pressure and δ=0 for compressible flow. The parameter θ is defined as

$$\theta = (1/U_r^2) - (\rho_T H + \rho C_p) \quad (4)$$

In Eq.(4), the reference velocity U_r is chosen such that the eigenvalues of the system remain well conditioned with respect to the convective and diffusive timescales, and C_p is the specific heat at constant pressure.

Two-equation, standard k-ε model, which is modified to take account for compressibility effect, is employed to close the governing equations. The turbulent model for μ_t is written by $\mu=\rho C_\mu(\kappa^2/\varepsilon)$, where the turbulent kinetic energy k and dissipation rate ε are solved from the turbulent transport theory. The standard model constants are used:

$$C_\mu=0.09,\ C_{1\varepsilon}=1.44,\ C_{2\varepsilon}=1.92,\ \sigma_\varepsilon=1.3,\ \sigma_k=1.0. \quad (5)$$

A preconditioning method to obtain more accurate velocity and pressure gradients in the flux terms. The advantage of the preconditioning allows the propagation of any acoustic waves in the system to be singled out.

The preconditioned governing equations are discretized spatially using a finite volume scheme, in which the physical domain is subdivided into numerical cells and the integral equations are applied to each cell. The flow field is represented by associating a distinct value of the discretized solution vector with each control volume,

which is used to evaluate the fluxes at cell faces. The solution vector is computed using a multidimensional linear reconstruction approach, which enables a higher-order accuracy to be achieved at the cell faces through a Taylor series expansion of the cell-averaged solution vector.

With respect to temporal discretization, an explicit multi-stage time stepping scheme is used to descretize the time derivatives in the governing equations. Then the solution is advanced from time t to time t+Δt with a multi-stage Runge-Kutta scheme. Using a second order accurate scheme makes it feasible to capture the shock structure around the orifices and the wake flow downstream of the orifice, but only with fine computational grids in the vicinity of the shock and wake flow. A multigrid scheme was used to accelerate the convergence of the solution on a series of coarse grid levels.

A convergence criterion of the solutions was established when the residuals for each of the conserved variables have reduced below the order of magnitude of 3. The residual of a variable is, in definition, the correction between the current iteration and the previous divide by the local time step. This merely means the time rate of change of the conserved variables. Some of the present computations showed that the residuals rose again, even after dropping below this convergence criterion so that further iterations were required for the converged solutions. This requires another convergence criterions for the correct solutions. The net mass flux through the computational boundaries was investigated if there were an applicable imbalance through the boundaries. These criteria served as a monitor for the converged solutions throughout the present computations.

The boundary conditions used were inlet total and static pressures and outlet static pressure. For subsonic flow at the outlet the pressure outlet condition requires only a static pressure specification at the pipe exit. If the flow is supersonic at the outlet boundary then the pressure is extrapolated from the interior with all other flow variables always being extrapolated regardless of local pressure fluctuations because of a hyperbolic nature of the supersonic flow.

The values of turbulent kinetic energy k and turbulent dissipation rate e are usually determined from the inlet flow velocity, turbulence intensity, and characteristic length scale of the flow, and should be specified on the boundaries. These values are typically in the range of 1% to 10%, closely depending on the flow configuration used. However in the present computations it is very unlikely that the choice of these values significantly affect the final solutions obtained.

The static pressure (P_a) at the exit of pipe was kept constant 101.3kPa and the air temperature at the inlet was kept 300K. Adiabatic, no slip wall and symmetry conditions were assumed on the pipe wall and the axis of the pipe, respectively. The total pressure (P_{ot}) at the inlet of the pipe was changed to give different values of pot/pa, which will be used as the operating pressure ratio.

3. Results and Discussion

Unlike the orifice system which has been usually applied to incompressible pipe flows, shock wave system can play an important role in effective silencer design of high-speed exhaust gas, because a considerably large part of flow energy would dissipate across it. Figure 3 shows Mach number contours of a double orifice system. The interval between orifices and the orifice area ratio were kept constant by l/R=1.50 and A_2/A_1=1.0, respectively. For the operating pressure ratio of P_{ot}/P_a=1.5, as shown in Figure 3(a), the flow remains subsonic throughout the whole flow in pipe. The shear layers from the edge of the first orifice impinge the second orifice, and there are the strong vortical flows between the orifices, as usually observed in a subsonic cavity flow.[9] The flow energy dissipates across the double orifice system. A quite wide range of separation region is observed downstream of the second orifice.

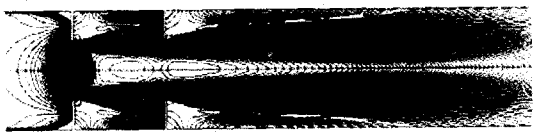

(a) $P_{ot}/P_a = 1.5$

(b) $P_{ot}/P_a = 4.0$

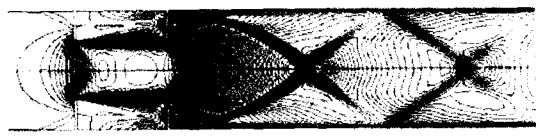

(c) $P_{ot}/P_a = 20.0$

Figure 3. Mach number contours for different operating pressure ratio (l/R = 1.5 and A_2/A_1 = 1.0)

For P_{ot}/P_a=4.0, as shown in Figure 3(b), the flow chokes at the second orifice and accelerates to a supersonic speed, consequently leading to the normal shock wave downstream of the second orifice. The normal shock wave interacts with the barrel shock of the supersonic jet stream, resulting in a reflected shock wave. A triple point forms at the location where these three shock waves meet each other. The flow decelerates to a subsonic speed through the normal shock but still remains supersonic when it passes through both the barrel shock and reflected shock waves. A slip flow generates between two streams, as observed just downstream of the

triple point. With a further increase in P_{ot}/P_a, the barrel shock wave leads to regular reflection on the pipe axis, and the resulting oblique shock system repeats up to far downstream of the second orifice. In this case, the separation region seems to be relatively small, compared with that observed in lower pressure ratio. Most of energy losses of the pipe flow generate through the successive shock system.

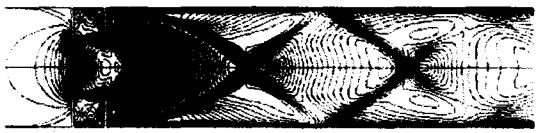

(a) $l/R = 0.5$

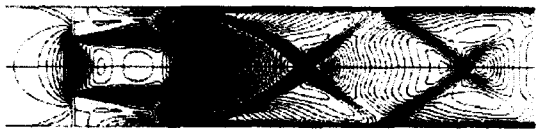

(b) $l/R = 1.5$

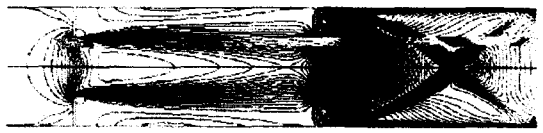

(c) $l/R = 4.0$

Figure 4. Mach number contours for different l/R values
($P_{ot}/P_a = 8.0$ and $A_2/A_1 = 1.0$)

Figure 4 shows the influence of the orifice interval l/R that has on the pipe flow field. With a given P_{ot}/P_a =8.0 and A_2/A_1=1.0, the shock structure downstream of the second orifice seems not to significantly change with the orifice interval. However the flow chokes at the second orifice regardless of the orifice interval. For l/R=4.0,the flow field is similar to a single orifice flowith the corresponding pressure ratio.

For P_{ot}/P_a=20.0 and l/R=2.5, Figure 5 shows Mach number contours with different orifice area ratio. With A_2/A_1=0.64, the second orifice area is larger than the first orifice area, and the flow always chokes at the second orifice. The shock structures, which are observed downstream of the second orifice, are nearly the same to those shown in Figure 4. With A_2/A_1=1.44, the flow always chokes at the first orifice and some weak normal shock waves are observed at the region between the first and second orifices. The shock structures downstream of the second orifice are qualitatively the same to those of Figure 5(b), but some difference is found in the shock strength. The strengths of the repeated shock waves are somewhat weaker, compared with those for A_2/A_1=0.64.

With A_2/A_1=2.56, a quite strong normal shock wave appears between the two orifices. The normal shock results from the reflection of the barrel shock on the pipe axis. The slip flow can also be observed downstream of the triple point and points toward the pipe axis. The supersonic flow locally decelerates to a subsonic speed across the normal shock wave, but the flow outside the slip stream still remains supersonic. There are strong shear actions between these two streams. This leads to reacceleration of the subsonic stream passing through the normal shock. The resulting flow, which is observed downstream of the second orifice, is qualitatively similar to that of Figure 5 (b). However each shock structure consisting of the repeated shock waves is different from that of Figure 5(b). Downstream of the second orifice, the first shock wave reflects on the pipe axis to form a normal shock, consequently leading to a subsonic flow just behind the normal shock. The second shock wave seems to be weaker, compared with that of Figure 5(b). In this case supersonic and subsonic flows repeats along the pipe axis.

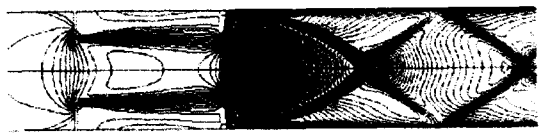

(a) $A_2/A_1 = 0.64$

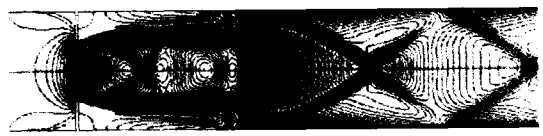

(b) $A_2/A_1 = 1.44$

(c) $A_2/A_1 = 2.56$

Figure 5. Mach number contours for different orifice area ratio
($P_{ot}/P_a = 20.0$ and $l/R = 2.5$)

Figure 6 shows Mach number contours for single, double and triple orifice systems. The orifice area ratio $A_2/A_1$and the orifice interval l/R were kept constant by 1.0 and 2.5, respectively. For the operating pressure ratio of 12.0, the single orifice flow shows the successive oblique shock systems, continuing up to far downstream of the orifice. For the double orifice flow the shock structure is different from that of the single orifice. There are weak wavelets between orifices, and the shock structure has a triple point downstream of the second

orifice. A strong slip stream results from the triple point of the shock structure, and continues up to far downstream of the triple point. In this case, the second shock system is very weak and is not observed clearly. In the triple orifice system, the flow always chokes at the third orifice where shock structure is nearly similar to that of the single orifice flow.

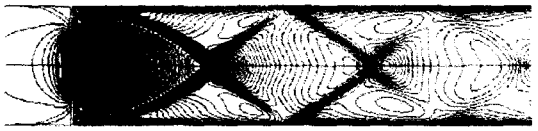

(a) Single orifice

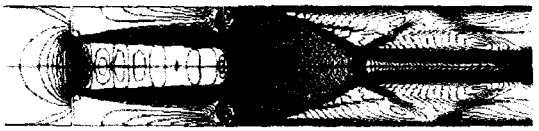

(b) Double orifice

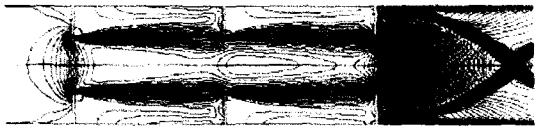

(c) Triple orifice

Figure 6. Mach number contours for different single, double, and triple orifice systems (P_{ot}/P_a = 12.0, l/R = 2.5, and A_2/A_1 = 1.0)

Figure 7 represents the relationship between the orifice interval l/R and the total pressure drop across the orifice system, where P_{ot} and P_{oe} are the inlet and outlet total pressures, respectively. The orifice area ratio was fixed constant by 1.0. With a low pressure ratio of P_{ot}/P_a=1.5, the flow is subsonic throughout the whole orifice system. The total pressure drop does not depend on the orifice intervals and is much smaller compared with higher pressure ratio. In this case, the total pressure drop would be caused by the viscous dissipations which largely generate between the orifices.

The total pressure drop increases with the operating pressure ratio but does not still strongly depend on the orifice intervals, although the total pressure drop for P_{ot}/P_a=20.0 is somewhat increased with the orifice intervals. Here it should be noted that the total pressure drop in low operating pressure ratio flows is about 32% of the inlet total pressure, while in high operating pressure ratio flows about 70% of the inlet total pressure. This high total pressure drop would result from the compressibility effects throughout the orifice flow.

Figure 8 shows the effect of the orifice area ratio on the total pressure drop in double orifice pipe flow. For P_{ot}/P_a=1.5, there seems to be no any dependency of the orifice area ratio on the total pressure drop. However the effect of the orifice area ratio becomes remarkable with the operating pressure ratio. The total pressure drop shows a peak value at A_2/A_1=1.0 and then has a minimum value at A_2/A_1=2.0 before increasing with a further increase in the orifice area ratio. For the double orifice system to reduce the pressure level of an exhaust gas, it is desirable to use the high orifice area ratio above 2.5. From both the data of P_{ot}/P_a=8.0 and 20.0, the total pressure drop characteristics seems to be nearly the same. This implies that the present CFD data could be used for the operating pressure ratios higher than those applied to the present study.

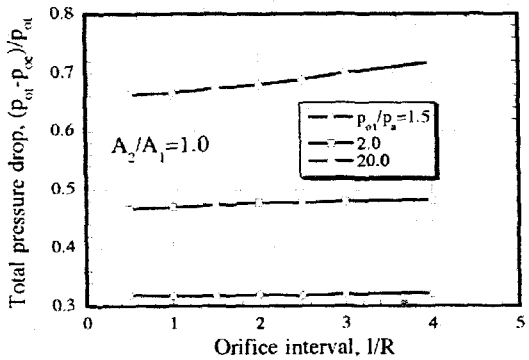

Figure 7. Effect of orifice interval on total pressure drop

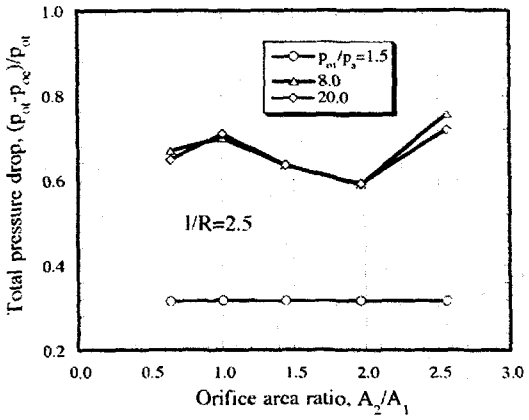

Figure 8. Effect of orifice area ratio on total pressure drop

Figure 9 represents the relationship between the total pressure drop and the operating pressure ratio. The orifice interval and the orifice area ratio are constant by 2.5

and 1.0 respectively. The total pressure drop rapidly increases when the operating pressure ratio increases from 1.5 to 4.0, but there is no remarkable difference with the number of orifice applied. The total pressure drop remains nearly constant for the further increase in the operating pressure ratio.

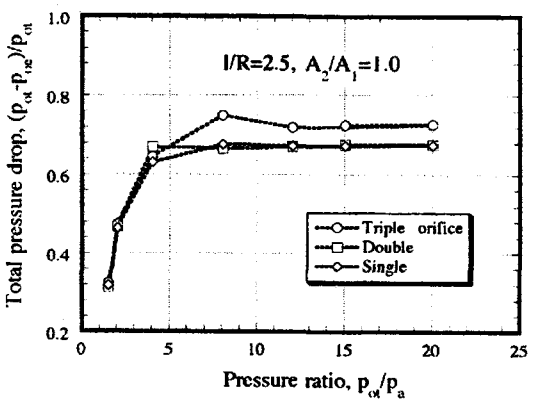

Figure 9. Effect of the operating pressure ratio on total pressure drop

The triple orifice system leads to a little larger pressure drops, compared with the single and double orifice systems. The total pressure drops for P_{ot}/P_a>4.0 are more than two times those for P_{ot}/P_a=1.5. The present CFD data show that the orifice systems, which have been applied to incompressible flow regime to date, can not be used for the high operating pressure ratio flows. Compressibility effect is the main reason for this difference.

4. Concluding Remark

In order to investigate the effectiveness of an orifice system in producing pressure drops and the effect of compressibility on the pressure drop, computations using the mass-averaged implicit Navier-Stokes equations were applied to the axisymmetric pipe flows with the operating pressure ratio from 1.5 to 2.0. The governing equations were discretized in space using a finite volume differencing formulation. The standard k-e turbulence model was employed to close the governing equations. Numerical calculations were carried out for some combinations of the multiple orifice configurations. The present CFD data showed that the orifice systems, which have been applied to incompressible flow regime to date, could not be used for the high operating pressure ratio flows. The orifice interval did not strongly affect the total pressure drop, but the orifice area ratio more than 2.5 led to higher pressure drops, when compared with the orifice area ratios below 2.5. The total pressure drop rapidly increased in the range of the operating pressure ratio from 1.5 to 4.0, but it did not to depend on the operating pressure ratio.

References

(1) Benedict, R.P., 1983, "Fundamentals of Gas Dynamics," John Wiley & Sons, Inc., Chap.4.

(2) James, R., 1965, "Metering of Steam-Water Two-Phase Flow by Sharp-Edged Orifices," Proc. Inst. Mech. Engrs., Vol.180, No.23, pp.549-566.

(3) Chisholm, D., 1977, "Two-Phase Flow through Sharp-Edged Orifices," J. Mech. Eng. Science, Vol.19, No.3, pp.128-130.

(4) Kim, H.D., Kim, T.H. and Woo, S.H., 1997, "Analytical Study on the Compressible Flow Through a Double Orifice," Korean Society of Propulsion Engineers Jour., Vol.1, No.2.

(5) Anderson, A., 1992, "A Note on Compressible Flow through Orifices in Series," Journal of Mechanical Engineering Science, Vol.206, pp.361-366.

(6) Mori,Y., Hijikata,K. and Shimizu,T., 1975, "Attenuation of Shock Wave by Multi-Orifice," 10th International Symp. Shock Tube & Waves.

(7) Yudin, E.Y., 1955, "The Acoustic Power of the Noise Created by Airduct Elements," Soviet Phys. Acoust., Vol.1, pp.383-398.

(8) Davis, D.D., Skokes, G.M., Moore, D. and Stevens, G.L., 1964, "Theoretical and Experimental Investigation of Mufflers with Comments on Engine-Exhaust Muffler Design," NACA Report 1192.

(9) Rossiter, J.E., 1964, "Wind Tunnel Experiments on the Flow over Rectangular Cavities at Subsonic and Transonic Speeds," Aeronautical Research council R & M No 3438.